

ISSN: 0256-307X

中国物理快报

Chinese Physics Letters

Volume 32 Number 10 October 2015

A Series Journal of the Chinese Physical Society
Distributed by IOP Publishing

Online: <http://iopscience.iop.org/0256-307X>
<http://cpl.iphy.ac.cn>

CHINESE PHYSICAL SOCIETY
IOP Publishing

JUST FOR AUTHORS
— CHINESE PHYSICS LETTERS

Trapping and Cooling of Single Atoms in an Optical Microcavity by a Magic-Wavelength Dipole Trap *

LI Wen-Fang(李文芳), DU Jin-Jin(杜金锦), WEN Rui-Juan(文瑞娟),
LI Gang(李刚), ZHANG Tian-Cai(张天才)**

State Key Laboratory of Quantum Optics and Quantum Optics Devices, Institute of Opto-Electronics,
Shanxi University, Taiyuan 030006

(Received 19 June 2015)

We present trapping and cooling of single cesium atoms inside a microcavity by means of an intracavity far-off-resonance trap (FORT). By the ‘magic’ wavelength FORT, we achieve state-insensitive single-atom trapping and cooling in a microcavity. The cavity transmission of the probe beam strongly coupled to single atoms enables us to continuously observe the intracavity atom trapping. The average atomic localization time inside the bright FORT is about 7 ms by introducing cavity cooling with appropriate detuning. This experiment presents great potential in coherent state manipulation for strongly coupled atom–photon systems in the context of cavity quantum electrodynamics.

PACS: 42.50.Pq, 37.10.De, 37.10.Gh, 37.30.+i

DOI: 10.1088/0256-307X/32/10/104210

Experimental physicists have made great strides toward the long-standing goal of producing a well-confined, isolated, and manipulable individual particle.^[1] The use of cavity quantum electrodynamics (QED), where an identified single mode in a high-finesse optical cavity couples to a single atom to probe matter-light interactions at the single quanta level, is one candidate that is able to achieve this goal.^[2,3] Cavity QED also offers unique advantages for precision measurement and quantum information science applications due to the fact that it provides the possibility of realizing complex quantum networks.^[4] The fundamental unit is possibly constructed by single trapped atoms strongly coupled to an optical cavity in the optical frequency regime. The system can be expanded when each atom acts as a network node and the whole system is linked together by optical fiber interconnects.^[5–7] To construct such a quantum node, a high quality resonator with small mode volume is required for the strong atom–cavity interaction, i.e., by demonstrating a reversible state mapping between atoms and photons with low dissipations.^[8] Another requirement is the development of experimental techniques to trap and localize atoms within a cavity in the strong coupling regime. Laser cooling and trapping techniques have been used widely, and diverse methods have been proposed to create the trapping potentials for various atom confinements over the past few decades. To date, the maximum dwell time of single atoms inside a microcavity has been extended to dozens of seconds.^[9] By means of ground state cooling of single atoms trapped in a three-dimensional optical lattice at the center of an optical cavity, Reiserer *et al.* have demonstrated full quantum control over the

internal state, position, and momentum of a single atom, and its coupling to the cavity field.^[10] The ability to fully control single atoms is important for many other systems such as the demonstration of quantum nondemolition detection for single photons,^[11] electromagnetically induced transparency (EIT) with single atoms in a cavity,^[12,13] nonlinear quantum optics at the level of individual atomic and photonic quanta.^[14,15]

Generally, additional far off-resonant trapping beams,^[16–19] near-resonant light with low intracavity photon numbers,^[20,21] and feedback control of single atoms^[22–24] are the main approaches to realize the above experiments. In particular, an FORT at the ‘magic’ wavelength has been used in a number of recent experiments to investigate precision quantum metrology for optical atomic clocks and coherent control of optical interactions of single atoms and photons within cavity QED.^[25] The magic FORT is able to separate internal and external dynamics well, which is critical for precision measurement, frequency metrology, and coherent manipulations of quantum systems.^[25] In this Letter, we experimentally demonstrate single-atom trapping in a micro-optical cavity using an intracavity far-off-resonance dipole-force trap and the interaction between the atom and cavity is in the strong coupling regime. The magic wavelength FORT laser provides state-insensitive cooling and trapping of single atoms in the cavity. The observed average lifetime is up to about 4 ms and the recorded maximum dwell time is about 40 ms, which is about 360 times longer than that without using the magic wavelength FORT. By monitoring the transmission of the probe laser through the cavity, this system

*Supported by the National Basic Research Program of China under Grant No 2012CB921601, and the National Natural Science Foundation of China under Grant Nos 11125418, 61121064, 61275210, 61227902 and 91336107.

**Corresponding author. Email: tczhang@sxu.edu.cn

© 2015 Chinese Physical Society and IOP Publishing Ltd

allows continuous observation of the atomic motion in the cavity mode. Through the cavity cooling mechanism, the average dwell time of single atoms in the cavity is doubled. This is an important step to lengthen the intracavity trapping time of a single atom from a few hundreds of microseconds to around 10 ms. With the longer duration time of an atom inside the microcavity, one can observe the dynamics of the trapped single-atom motion inside the higher-order transverse cavity modes and manipulate the quantum state of entangled atom-cavity system for research of various quantum behaviors.

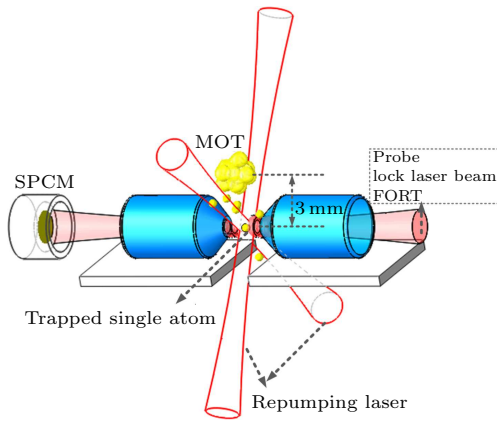


Fig. 1. (Color online) Experimental setup for single atom trapping and cooling within the cavity in the strong coupling regime. The cavity (blue) comprises two mirrors with a cavity length of about $86\ \mu\text{m}$. The input beams consist of FORT (for atom trapping), probe and locking beams. The single photon counting module (SPCM) is used to monitor cavity transmission. A magneto-optical trap is located at 3 mm above the center of the cavity.

The experimental setup is schematically depicted in Fig. 1. The Fabry-Pérot cavity with cavity length of about $86.8\ \mu\text{m}$ ^[26] is the central component for isolation and interaction with single atoms. The cavity consists of two super-polished spherical mirrors with a radius of curvature of 100 mm and an end diameter of 1 mm. The principle parameters of our cavity QED system are the Rabi frequency $2g_0$ for a single quantum of excitation and the decay rates κ, γ resulting from the cavity decay and cesium atomic spontaneous emission, respectively. Both g_0 and κ are determined by means of transmission of single atoms coupled to the cavity. These parameters for our microcavity are measured as $(g_0, \kappa, \gamma) = 2\pi \times (23.9, 2.6, 2.6)$ MHz for the TEM_{00} , where g_0 is the coupling strength for the transition of $6^2S_{1/2}, F=4 \rightarrow 6^2P_{3/2}, F'=5$ in a cesium atom at a wavelength of $\lambda_0 = 852.36\ \text{nm}$. Strong coupling between atom and cavity is thereby reached, i.e., $g_0 \gg (\kappa, \gamma)$, leading to critical atom and photon numbers $N_0 = 2\kappa\gamma/g_0^2 \simeq 0.024$, $m_0 = \gamma^2/(2g_0^2) \simeq 0.006$.

The horizontal input beam to the cavity is illustrated in Fig. 1 (see the red beam), which is made up of the FORT field, probe and locking beams,

which are all overlapped and eventually directed to the different detectors at the output separately. The probe light with $\lambda_0 = 852.36\ \text{nm}$ transmitted through the cavity is monitored by a single photon counting module (SPCM) allowing real-time detection of single cesium atoms within the cavity field.^[27–29] For the probe beam, the waist of intracavity TEM_{00} is $\omega_0 = 23.8\ \mu\text{m}$ and the finesse of the cavity is 3.3×10^5 . An external cavity diode laser (ECDL) working at a cavity resonance wavelength of $\lambda_C = 828\ \text{nm}$ is used for cavity locking and detuning control. To achieve state-insensitive trapping of single atoms while still maintaining strong coupling between atom and cavity for the cesium D_2 transition, we introduce the magic wavelength laser at $\lambda_F = 933.9\ \text{nm}$ as the intracavity FORT beam. The summation of ac-stark shifts from different allowed optical dipole transitions leads to both the ground and excited states shifted downwards by comparable amounts, which is shown in Fig. 2. The FORT beam caused detuning, which basically results in the effective couplings between single atoms and cavity mode being functions of the atomic position. However, magic wavelength FORT causes the same shift for upper and lower levels, which provides the possibility of realizing state-insensitive trapping and maintaining strong coupling for the D_2 transition of the cesium atom. The FORT is provided by another ECDL which is independently locked to the cavity. The finesse of the cavity at this wavelength is $F \approx 8600$ and the waist of the intracavity TEM_{00} is $\omega_F = 24.9\ \mu\text{m}$. Thus a mode-matched cavity output power of 0.5 mW provides a trap with the depth of $U_0/k_B \approx 5.4\ \text{mK}$. Both the probe and FORT beams are linearly polarized along a direction that is orthogonal to the axis of the cavity.

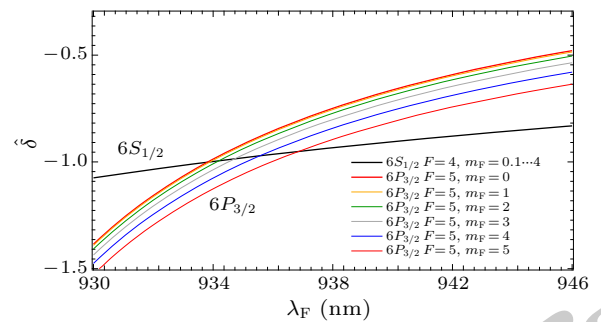


Fig. 2. (Color online) The ac-stark shift ($6\delta_{6S_{1/2}}, 6\delta_{6P_{3/2}, F'=5}$) as a function of wavelength λ_F for the ($6S_{1/2}, 6P_{3/2}$) levels of cesium for a linearly polarized FORT. The normalization parameter is defined as $\delta = |\delta/\delta_{6S_{1/2}}(\lambda_F = 933.9\ \text{nm})|$.

Roughly 1×10^5 atoms are collected by a magneto-optical trap (MOT) in a UHV chamber operating at a background pressure of about 1×10^{-10} Torr, which is located about 3 mm above the center of the cavity. After a polarization gradient cooling phase, the temperature of cold atoms is down to $30\ \mu\text{K}$.^[28] Then, as

soon as the trapping laser beams and magnetic field are switched off, the atoms fall freely under gravity. Freely falling atoms arrive at the cavity center over an interval of about 10 ms with the average kinetic energy $\langle E_K/k_B \rangle \approx 0.4$ mK, mean velocity $\langle \nu \rangle \approx 0.2$ m/s, and average transit time $\Delta t = 2\omega_0/\nu \approx 120$ μ s. Two additional orthogonal pairs of counter-propagating repumping laser beams are located perpendicular to the cavity axis in the horizontal direction (see red beams in Fig. 1.). These beams near the $6^2S_{1/2}, F = 3 \rightarrow 6^2P_{3/2}, F' = 3$ transition are used to counteract the atomic velocity from the free-fall motion and to provide the possibility of trapping atoms in the FORT.

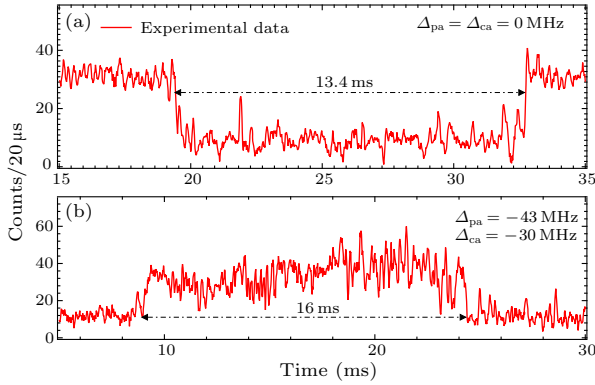


Fig. 3. The recorded atom trapping signals by the SPCM either at resonance (a) or with some detunings (b).

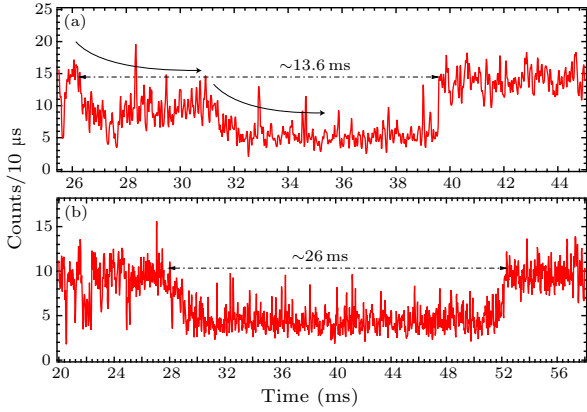


Fig. 4. The recorded atom trapping signals containing information about single atoms motion in the cavity: (a) the dwell time about 13.6 ms, and (b) about 26 ms.

The detection of typical single atoms trapped within the cavity mode is illustrated in Fig. 3. Two separate trapped atom events are presented by continuous observation under different detunings between the cavity or probe laser and the atom. For an example, the arrival of an atom at the cavity mode is sensed by observing an obvious reduction of the probe transmission, and we can see that the atom is trapped by the FORT at the magic wavelength with a dwell time of about 13.4 ms when the cavity mode is on resonance ($\Delta_{pa} = \omega_p - \omega_a = 0$ MHz, $\Delta_{ca} = \omega_c - \omega_a = 0$ MHz), where ω_p , ω_a , ω_c denote the probe, atom transition, and cavity frequencies, respectively. The second event

was recorded with detunings of $\Delta_{pa} = -43$ MHz and $\Delta_{ca} = -30$ MHz, and for this case, the transmission of the cavity remains at a low level in the absence of an atom and reaches a higher level once an atom is trapped inside the cavity. The dwell time is about 16 ms. It should be noted that the repumping beams play an important role in cooling atoms. Without this repumping light the atoms will fall into the cavity and then fly out from the near conservative FORT. In the absence of the repumping laser, single atoms could not be trapped in the cavity. We can not only obtain the dwell time of single atoms from the recorded transmission spectra but also know information about the motion of single atoms inside the cavity mode like Fig. 4. In theory, the axial and radial oscillations can be clearly observed by the photon correlation function.^[30] However, it does not work here due to the fact that the time intervals between our data points are not spaced closely enough to observe, resulting from the limited signal-to-noise ratio for our system.

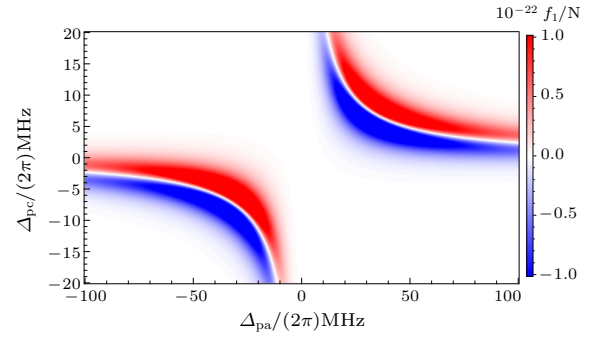


Fig. 5. Friction force f_1 for an intracavity atom. Heating and cooling regions are indicated by red and blue colors, respectively. The detunings are defined as $\Delta_{ac} = \omega_a - \omega_c$ and $\Delta_{pc} = \omega_p - \omega_c$. The parameters of our cavity are $(g_0, \kappa, \gamma) = 2\pi \times (23.9, 2.6, 2.6)$ MHz and the intracavity photon number is about 1.

Single atoms strongly coupled to a high finesse cavity allows cooling of the atoms by the cavity cooling mechanism,^[31–33] which can improve the performance of atom–cavity systems for quantum information processing. Theoretical investigation has indicated the importance of proper selection of the friction coefficient, which governs the intracavity atom to be either in the cooling or heating regions. The total friction force f_1 is determined by the detunings^[34] and the expression for the force f_1 can be found in appendix A of Ref. [34]. We have shown the force f_1 of the single atom in Fig. 5 as a function of both detunings $\Delta_{pc} = \omega_p - \omega_c$ and $\Delta_{pa} \equiv \omega_p - \omega_a$ with the parameters (g , κ and γ) corresponding to our system. Considering the signal-to-noise ratio of the SPCM and the region of cavity cooling, we choose $\Delta_{pc} = 0$ MHz and $\Delta_{ac} = 25$ MHz to further extend the intracavity dwell time.

The average dwell time of an atom in the presence

of probe beams (bright trap) is statistically obtained by recording the atom trapping signals. The result is shown in Fig. 6. The dwell time of single atoms in the cavity is about 3.7 ± 0.2 ms without cavity cooling and is extended to 6.8 ± 0.9 ms by cavity cooling (see Fig. 6). Note that the probe laser is always on during the loading stage of the dipole trap, leading to the occurrence of light-induced heating and then the creation of an additional loss channel.^[35] In principle, the lifetime of an atom in a dark trap should be longer by reducing or switching off the intensity of the probe laser.^[16,33]

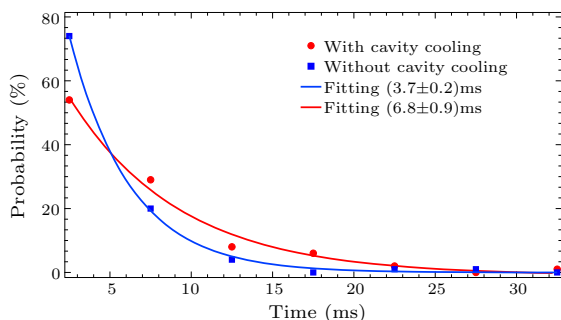


Fig. 6. The average dwell time in the cavity for two cases: without cavity cooling (blue squares) and with cavity cooling (red dots). The solid lines are exponential fits that yield dwell times of 3.7 ± 0.2 ms and 6.8 ± 0.9 ms, respectively.

In summary, we have described in detail a state-insensitive single-atom trap in an optical cavity by means of an intracavity magic wavelength FORT in a strong coupling cavity QED system. This FORT can eliminate the relative ac-stark shift between the ground and excited states, resulting in state-insensitive trapping and cooling of single atoms in the cavity. In our system the intracavity dwell time for single atoms can be extended to as long as 3.7 ± 0.2 ms, which is much longer than that with no FORT at all. By cavity cooling mechanism the dwell time can be further increased to 6.8 ± 0.9 ms by the optimized detunings. The final dwell time is limited by the fluctuations of light forces of the far-detuned intracavity field and various technical noises in the experiment. Long-time trapping single atoms within a cavity is important for realizing coherent state manipulation of single atoms in strongly coupled atom-cavity QED systems and quantum information.

References

- [1] Haroche S 2013 *Rev. Mod. Phys.* **85** 1083
- [2] Kimble H J 1998 *Phys. Scr.* **T76** 127
- [3] Berman P 1994 *Cavity Quantum Electrodynamics* (New York: Academic Press)
- [4] Kimble H J 2008 *Nature* **453** 1023
- [5] Cirac J I, Zoller P, Kimble H J and Mabuchi H 1997 *Phys. Rev. Lett.* **78** 3221
- [6] Ritter S, Nolleke C, Hahn C, Reiserer A, Neuzner A, Uphoff M, Mcke M, Figueroa E, Bochmann J and Rempe G 2012 *Nature* **484** 195
- [7] Specht H P, Nolleke C, Reiserer A, Uphoff M, Figueroa E, Ritter S and Rempe G 2011 *Nature* **473** 190
- [8] Hijlkema M, Weber B, Specht H P, Webster S C, Kuhn A and Rempe G 2007 *Nat. Phys.* **3** 253
- [9] Nubmann S, Murr K, Hijlkema M, Weber B, Kuhn A and Rempe G 2005 *Nat. Phys.* **1** 122
- [10] Reiserer A, Nolleke C, Ritter S and Rempe G 2013 *Phys. Rev. Lett.* **110** 223003
- [11] Reiserer A, Ritter S and Rempe G 2013 *Science* **342** 1349
- [12] Mücke M, Figueroa E, Bochmann J, Hahn C, Murr K, Ritter S, Villas-Boas C J and Rempe G 2010 *Nature* **465** 755
- [13] Souza J A, Figueroa E, Chibani H, Villas-Boas C J and Rempe G 2013 *Phys. Rev. Lett.* **111** 113602
- [14] Schuster I, Kubanek A, Fuhrmanek A, Puppe T, Pinkse P W H, Murr K and Rempe G 2008 *Nat. Phys.* **4** 382
- [15] Kubanek A, Ourjountsev A, Schuster I, Koch M, Pinkse P W H, Murr K and Rempe G 2008 *Phys. Rev. Lett.* **101** 203602
- [16] Ye J, Vernooij D W and Kimble H J 1999 *Phys. Rev. Lett.* **83** 4987
- [17] Sauer A, Fortier K M, Chang M S, Hamley C D and Chapman M S 2004 *Phys. Rev. A* **69** 051804(R)
- [18] McKeever J, Buck J R, Boozer A D, Kuzmich A, Nagerl H C, Stamper-Kurn D M and Kimble H J 2003 *Phys. Rev. Lett.* **90** 133602
- [19] Li G, Zhang S, Isenhower L, Maller K and Saffman M 2012 *Opt. Lett.* **37** 851
- [20] Hood C J, Lynn T W, Doherty A C, Parkins A S and Kimble H J 2000 *Science* **287** 1447
- [21] Pinkse P W H, Fischer T, Maunz P and Rempe G 2000 *Nature* **404** 365
- [22] Kubanek A, Koch M, Sames C, Ourjountsev A, Pinkse P W H, Murr K and Rempe G 2009 *Nature* **462** 898
- [23] Fischer T, Maunz P, Pinkse P W H, Puppe T and Rempe G 2002 *Phys. Rev. Lett.* **88** 163002
- [24] Kubanek A, Koch M, Sames C, Ourjountsev A, Wilk T, Pinkse P W H and Rempe G 2011 *Appl. Phys. B* **102** 433
- [25] Ye J, Kimble H J and Katori H 2008 *Science* **320** 1734
- [26] Zhang P F, Zhang Y C, Li G, Du J J, Zhang Y F, Guo Y Q, Wang J M, Zhang T C and Li W D 2011 *Chin. Phys. Lett.* **28** 044203
- [27] Du J J, Li W F, Wen R J, Li G, Zhang P F and Zhang T C 2013 *Appl. Phys. Lett.* **103** 083117
- [28] Li W F, Du J J, Wen R J, Li G, Yang P F, Liang J J and Zhang T C 2014 *Appl. Phys. Lett.* **104** 113102
- [29] Zhang P F, Guo Y Q, Li Z H, Zhang Y C, Zhang Y F, Du J J, Li G, Wang J M and Zhang T C 2011 *Phys. Rev. A* **83** 031804(R)
- [30] Maunz P 2004 *Cavity Cooling and Spectroscopy of a Bound Atom-Cavity System* (PhD dissertation) (Garching: Max-Planck-Institute of Quantum Optics)
- [31] Horak P, Hechenblaikner G, Gheri K M, Stecher H and Ritsch H 1997 *Phys. Rev. Lett.* **79** 4974
- [32] Leibbrandt D R, Labaziewicz J, Vuletic V and Chuang I L 2009 *Phys. Rev. Lett.* **103** 103001
- [33] Maunz P, Puppe T, Schuster I, Syassen N, Pinkse P W H and Rempe G 2004 *Nature* **428** 50
- [34] Hechenblaikner G, Gangl M, Horak P and Ritsch H 1998 *Phys. Rev. A* **58** 3030
- [35] Weiner J and Julienne P S 1999 *Rev. Mod. Phys.* **71** 1

Chinese Physics Letters

Volume 32

Number 10

October 2015

GENERAL

- 100301 An Efficient Multiparty Quantum-State Sharing Scheme**
QIN Hua-Wang, DAI Yue-Wei
- 100302 Motion of a Nonrelativistic Quantum Particle in Non-commutative Phase Space**
FATEME Hoseini, MA Kai, HASSAN Hassanabadi
- 100303 Quantum Correlations in Ising-XYZ Diamond Chain Structure under an External Magnetic Field**
Faizi E., Eftekhari H.
- 100401 On Hawking Radiation of 3D Rotating Hairy Black Holes**
Belhaj A., Chabab M., El Moumni H., Masmarr K., Sedra M. B.
- 100501 Optimal Performance Analysis of a Three-Terminal Thermoelectric Refrigerator with Ideal Tunneling Quantum Dots**
SU Hao, SHI Zhi-Cheng, HE Ji-Zhou
- 100701 A Longitudinal Zeeman Slower Based on Ring-Shaped Permanent Magnets for a Strontium Optical Lattice Clock**
WANG Qiang, LIN Yi-Ge, GAO Fang-Lin, LI Ye, LIN Bai-Ke, MENG Fei, ZANG Er-Jun, LI Tian-Chu, FANG Zhan-Jun

THE PHYSICS OF ELEMENTARY PARTICLES AND FIELDS

- 101101 Tunneling of Relativistic Bosons Induced by Magnetic Fields in the Magnetar's Crust**
Marina-Aura Dariescu, Ciprian Dariescu, Denisa-Andreea MiHu
- 101201 Identification of $Y(4008)$, $Y(4140)$, $Y(4260)$, and $Y(4360)$ as Tetraquark States**
ZHOU Ping, DENG Cheng-Rong, PING Jia-Lun

FUNDAMENTAL AREAS OF PHENOMENOLOGY(INCLUDING APPLICATIONS)

- 104201 High-Power Dual-End-Pumped Actively Q-Switched Ho:YAG Ceramic Laser**
DUAN Xiao-Ming, YUAN Jin-He, YAO Bao-Quan, DAI Tong-Yu, LI Jiang, PAN Yu-Bai
- 104202 Light Focusing through Scattering Media by Particle Swarm Optimization**
HUANG Hui-Ling, CHEN Zi-Yang, SUN Cun-Zhi, LIU Ji-Lin, PU Ji-Xiong
- 104203 High-Power and High-Efficiency Operation of Terahertz Quantum Cascade Lasers at 3.3 THz**
LI Yuan-Yuan, LIU Jun-Qi, WANG Tao, LIU Feng-Qi, ZHAI Shen-Qiang, ZHANG Jin-Chuan, ZHUO Ning, WANG Li-Jun, LIU Shu-Man, WANG Zhan-Guo
- 104204 Polarization Stable Vertical Cavity Surface Emitting Laser Array Based on Proton Implantation**
XUN Meng, XU Chen, XIE Yi-Yang, DENG Jun, XU Kun, JIANG Guo-Qing, PAN Guan-Zhong, CHEN Hong-Da
- 104205 Efficient Passively Q-Switched Nd:YAG/Cr⁴⁺:YAG/LBO Microchip Laser**
FU Sheng-Gui, OUYANG Xue-Ying, LIU Xiao-Juan
- 104206 Surface Plasmon Interference Lithography Assisted by a Fabry-Perot Cavity Composed of Subwavelength Metal Grating and Thin Metal Film**
LIANG Hui-Min, WANG Jing-Quan, WANG Xue, WANG Gui-Mei
- 104207 Attosecond-Resolution Er:Fiber-Based Optical Frequency Comb**
YAN Lu-Lu, ZHANG Yan-Yan, ZHANG Long, FAN Song-Tao, ZHANG Xiao-Fei, GUO Wen-Ge, ZHANG Shou-Gang, JIANG Hai-Feng
- 104208 Cr²⁺:ZnS Saturable Absorber Passively Q-Switched Ho:LuVO₄ Laser**
CUI Zheng, YAO Bao-Quan, DUAN Xiao-Ming, BAI Shuang, LI Jiang, YUAN Jin-He, DAI Tong-Yu, LI Chao-Yu, PAN Yu-Bai

- 104209 **Heptad Phase Vortex Array in Extremely Deep Fresnel Diffraction Region Generated by Asymmetrical Metal Subwavelength Holes Film**
JIANG Shu-Na, LI Xing, MA Li, GAO Ya-Ru, GUI Wei-Ling, CHENG Chuan-Fu
- 104210 **Trapping and Cooling of Single Atoms in an Optical Microcavity by a Magic-Wavelength Dipole Trap**
LI Wen-Fang, DU Jin-Jin, WEN Rui-Juan, LI Gang, ZHANG Tian-Cai
- 104401 **Thermal Transport in Methane Hydrate by Molecular Dynamics and Phonon Inelastic Scattering**
WANG Zhao-Liang, YUAN Kun-Peng, TANG Da-Wei

PHYSICS OF GASES, PLASMAS, AND ELECTRIC DISCHARGES

- 105201 **MF-DFA Analysis of Turbulent Transport Measured by a Multipurpose Probe**
Lafouti M., Ghoranneviss M.

CONDENSED MATTER: STRUCTURE, MECHANICAL AND THERMAL PROPERTIES

- 106101 **Magneto-Caloric Response of a $Gd_{55}Co_{25}Al_{18}Sn_2$ Bulk Metallic Glass**
DING Ding, ZHANG Yi-Qing, XIA Lei
- 106201 **External-Strain-Induced Raman Scattering Modification in $g-C_3N_4$ Structures**
LI Ting-Hui, LI Hai-Tao, PAN Jiang-Hong, GUO Jun-Hong, HU Fang-Ren
- 106801 **Growth and Characterization of $InAs_{1-x}Sb_x$ with Different Sb Compositions on GaAs Substrates**
SUN Qing-Ling, WANG Lu, WANG Wen-Qi, SUN Ling, LI Mei-Cheng, WANG Wen-Xin, JIA Hai-Qiang, ZHOU Jun-Ming, CHEN Hong

CONDENSED MATTER: ELECTRONIC STRUCTURE, ELECTRICAL, MAGNETIC, AND OPTICAL PROPERTIES

- 107101 **Observation of Fermi Arcs in Non-Centrosymmetric Weyl Semi-Metal Candidate NbP**
XU Di-Fei, DU Yong-Ping, WANG Zhen, LI Yu-Peng, NIU Xiao-Hai, YAO Qi, Dudin Pavel, XU Zhu-An, WAN Xian-Gang, FENG Dong-Lai
- 107301 **Transport through a Single Barrier on Monolayer MoS_2**
CHENG Fang, REN Yi, SUN Jin-Fang
- 107302 **Wet Chemical Etching of Antimonide-Based Infrared Materials**
HAO Hong-Yue, XIANG Wei, WANG Guo-Wei, XU Ying-Qiang, REN Zheng-Wei, HAN Xi, HE Zhen-Hong, LIAO Yong-Ping, WEI Si-Hang, NIU Zhi-Chuan
- 107303 **Effect of Thermal Annealing on Light-Induced Minority Carrier Lifetime Enhancement in Boron-Doped Czochralski Silicon**
WANG Hong-Zhe, ZHENG Song-Sheng, CHEN Chao
- 107304 **Contact-Size-Dependent Cutoff Frequency of Bottom-Contact Organic Thin Film Transistors**
SUN Jing, WANG Hong, WANG Zhan, WU Shi-Wei, MA Xiao-Hua
- 107305 **Waveguide Mode Splitter Based on Multi-mode Dielectric-Loaded Surface Plasmon Polariton Waveguide**
CAI Yong-Jing, LI Ming, XIONG Xiao, YU Le, REN Xi-Feng, GUO Guo-Ping, GUO Guang-Can
- 107401 **New Superconductivity Dome in $LaFeAsO_{1-x}F_x$ Accompanied by Structural Transition**
YANG Jie, ZHOU Rui, WEI Lin-Lin, YANG Huai-Xin, LI Jian-Qi, ZHAO Zhong-Xian, ZHENG Guo-Qing
- 107801 **Polarization Insensitivity in Double-Split Ring and Triple-Split Ring Terahertz Resonators**
WU Qian-Nan, LAN Feng, TANG Xiao-Pin, YANG Zi-Qiang
- 107802 **Synthesis, Structure and Optical Properties of CdO Nanocrystals Directly Grown on Cd Foil**
LI Yong, LING Hong, GAO Lei, SONG Yue-Li, TIAN Ming-Li, ZHOU Feng-Qun
- 107803 ***Ab Initio* Study of the Dynamical Si–O Bond Breaking Event in α -Quartz**
SU Rui, ZHANG Hong, HAN Wei, CHEN Jun

- 107804 Au Microdisk-Size Dependence of Quantum Dot Emission from the Hybrid Metal-Distributed Bragg Reflector Structures Employed for Single Photon Sources**
WANG Hai-Yan, SU Dan, YANG Shuang, DOU Xiu-Ming, ZHU Hai-Jun, JIANG De-Sheng, NI Hai-Qiao, NIU Zhi-Chuan, ZHAO Cui-Lan, SUN Bao-Quan
- 107805 High-Performance Hybrid White Organic Light-Emitting Diodes Utilizing a Mixed Interlayer as the Universal Carrier Switch**
DING Lei, LI Huai-Kun, ZHANG Mai-Li, CHENG Jun, ZHANG Fang-Hui
- 107901 Fabrication of Through Micro-hole Arrays in Silicon Using Femtosecond Laser Irradiation and Selective Chemical Etching**
GAO Bo, CHEN Tao, CHEN Ying, SI Jin-Hai, HOU Xun

CROSS-DISCIPLINARY PHYSICS AND RELATED AREAS OF SCIENCE AND TECHNOLOGY

- 108101 Simple Method to Fabricate Au Nanoparticle-Decorated TiO₂ Nanotube Arrays for Enhanced Visible Light Photocurrent**
LU Yu-Hua, WANG Wen-Gui, WENG Yu-Yan, DONG Wen
- 108102 Fabrication and Piezoelectric Characterization of Single Crystalline GaN Nanobelts**
WU Dong-Xu, CHENG Hong-Bin, ZHENG Xue-Jun, WANG Xian-Ying, WANG Ding, LI Jia
- 108501 High-Efficiency Bottom-Emitting Organic Light-Emitting Diodes with Double Aluminum as Electrodes**
ZHANG Hong-Mei, WANG Dan-Bei, WU Yuan-Wu, FANG Da, HUANG Wei
- 108502 Statistical Modeling of Gate Capacitance Variations Induced by Random Dopants in Nanometer MOSFETs Reserving Correlations**
LÜ Wei-Feng, WANG Guang-Yi, LIN Mi, SUN Ling-Ling
- 108503 Quantum Coupling Effect between Quantum Dot and Quantum Well in a Resonant Tunneling Photon-Number-Resolving Detector**
WENG Qian-Chun, AN Zheng-Hua, XIONG Da-Yuan, ZHU Zi-Qiang
- 108701 Temperature Effects on Information Capacity and Energy Efficiency of Hodgkin–Huxley Neuron**
WANG Long-Fei, JIA Fei, LIU Xiao-Zhi, SONG Ya-Lei, YU Lian-Chun
- 108702 Improvements for Manipulating DNA with Optical Tweezers**
ZHU Chun-Li, LI Jing

GEOFYSICS, ASTRONOMY, AND ASTROPHYSICS

- 109501 Quintessence Cosmology with an Effective Λ -Term in Lyra Manifold**
Khurshudyan M., Pasqua A., Sadeghi J., Farahani H.

JUST FOR AUTHORS
— CHINESE PHYSICS LETTERS